RESEARCH ARTICLE

Integrating encounter theory with decision analysis to evaluate collision risk and determine optimal protection zones for wildlife

Bradley J. Udell[1] (iD)　|　Julien Martin[2] (iD)　|　Robert J. Fletcher Jr.[1] (iD)　|　Mathieu Bonneau[3] (iD)　|　Holly H. Edwards[4]　|　Timothy A. Gowan[4]　|　Stacie K. Hardy[4]　|　Eliezer Gurarie[5] (iD)　|　Charles S. Calleson[6]　|　Charles J. Deutsch[7]

[1]Department of Wildlife Ecology and Conservation, University of Florida, Gainesville, Florida; [2]US Geological Survey, Wetland and Aquatic Research Center, Gainesville, Florida; [3]Zootechnic Researchers (URZ, UR143), INRA 97170, Petit-Bourg (French West Indies), France; [4]Florida Fish and Wildlife Conservation Commission, Fish and Wildlife Research Institute, St. Petersburg, Florida; [5]Department of Biology, University of Maryland, College Park, Maryland; [6]U.S. Fish and Wildlife Service, Jacksonville, Florida and [7]Florida Fish and Wildlife Conservation Commission, Fish and Wildlife Research Institute, Gainesville, Florida

Correspondence
Bradley J. Udell
Email: bradjudell@ufl.edu

Abstract

1. Better understanding human–wildlife interactions and their links with management can help improve the design of wildlife protection zones. One example is the problem of wildlife collisions with vehicles or human-built structures (e.g., power lines, wind farms). In fact, collisions between marine wildlife and watercraft are among the major threats faced by several endangered species of marine mammals. Natural resource managers are therefore interested in finding cost-effective solutions to mitigate these threats.

2. We combined abundance estimators with encounter rate theory to estimate relative lethal collision risk of the Florida manatee (*Trichechus manatus latirostris*) from watercraft. We first modelled seasonal abundance of watercraft and manatees using a Bayesian analysis of aerial survey count data. We then modelled relative lethal collision risk in space and across seasons. Finally, we applied decision analysis and Linear Integer Programming to determine the optimal design of speed zones in terms of relative risk to manatees and costs to waterway users. We used a Pareto efficient frontier approach to evaluate the performance of alternative zones, which included additional practical considerations (e.g., spatial aggregation of speed zones) in relation to the optimal zone configurations.

3. Under the various relationships for probability of death given strike speed that we considered, the current speed zones reduced the relative lethal collision risk by an average of 51.5% to 70.0% compared to the scenario in which all speed regulations were removed (i.e., the no-protection scenario). We identified optimal zones and near-optimal zones with additional management considerations that improved upon the current zones in terms of cost or relative risk.

4. *Policy implications*. Our analytical framework combines encounter rate theory and decision analysis to quantify the effectiveness of speed zones in protecting manatees while accounting for uncertainty. Our approach can be used to optimize the

design of protection zones intended to reduce conflicts between human water-borne activity and marine mammals. This framework could be extended to address many other problems of human–wildlife interactions, such as the optimal placement of wind farms to minimize collisions with wildlife or the optimal allocation of ranger effort to mitigate poaching threats.

KEYWORDS

abundance, collision risk, encounter rate, Florida Manatee, human–wildlife interactions, marine mammals, protection zones

1 | INTRODUCTION

Conservation professionals are often interested in understanding and managing ecological interactions, especially interactions between humans and wildlife. Examples include limiting the impact of wind turbines on wildlife (Kunz et al., 2007) and establishing vessel speed regulations to reduce collisions with marine wildlife (Conn & Silber, 2013; Vanderlaan et al., 2009). Encounter rate theory provides a useful framework for modelling such interactions (Gurarie & Ovaskainen, 2013; Hutchinson & Waser, 2007; Koopman, 1956). Encounter rate theory was developed as an analytically tractable way to model the rate of encounter between mobile agents in space and time given their abundances, sizes, speeds, and area of interaction. It has broad applications in modelling many types of ecological interactions such as predator–prey, mate finding, dispersal, and pollination (Gerritsen & Strickler, 1977; Gurarie & Ovaskainen, 2013; Hutchinson & Waser, 2007). Recently, encounter rate theory has been applied to quantify the risk of collisions between marine mammals and watercraft (Martin et al., 2016).

One potential application of encounter rate theory stems from its integration with decision-support tools used for spatial conservation prioritization (e.g., Moilanen, Wilson, & Possingham, 2009). This integration could ultimately help managers improve the design of protection zones while considering the implications of animal movement and relevant interactions. For example, wildlife-vehicle collisions can have important impacts on protected species and can also affect human safety (Laist, Knowlton, Mead, Collet, & Podesta, 2001). By quantifying rates of encounters, application of this approach could facilitate formal spatial analysis of risk and potential human–wildlife conflicts within a protected area. Here, we show how to use encounter rate theory to determine the potential effectiveness of protection zones. We then demonstrate how to combine encounter rate theory with decision analysis to improve the design of these zones while considering both the risk of wildlife collisions and socioeconomic costs.

We illustrate our approach with a case study of collisions between Florida manatees (*Trichechus manatus latirostris*) and watercraft. Watercraft collisions are one of the largest sources of human-caused mortality for the federally protected Florida manatee (Runge et al., 2017). The establishment of protection zones to regulate the speed of watercraft is a primary management action taken to reduce manatee mortality (Calleson & Frohlich, 2007; USFWS, 2001); however, these protection zones may impose burdens on waterway users (Aipanjiguly, Jacobson, & Flamm, 2003). Linking management actions to risk of lethal collision is therefore desirable to evaluate and improve upon the effectiveness of such actions.

Martin et al. (2016) developed an approach to investigate the risk of lethal collision between wildlife and watercraft. They derived an analytical approach to determine encounter rates, which can be nested within a Bayesian Belief Network to account for probabilistic processes affecting risk of collision (e.g., the probability that a manatee is within strike depth and the probability of death given strike speed; see figure 1 in Martin et al., 2016). One advantage of including these parameters over simpler models (such as a co-occurrence approach; Bauduin et al., 2013) is the ability to incorporate more complexity into the collision process (e.g., the effect of boat speed on risk of deadly collisions). This approach also incorporates uncertainty in the estimate of relative risk, which allows one to calculate Bayesian credible intervals and quantify the probability that a given management scenario reduces relative risk. Other approaches include using individual-based simulations to estimate encounter rates between marine mammals and watercraft (van der Hoop, Vanderlaan, & Taggart, 2012), but such approaches can be computationally time consuming.

The abundance of animals and of boats is a critical parameter that must be modelled in space and time to implement this framework. As imperfect detection is a particularly problematic issue for marine mammals (Martin et al., 2015) we applied Bayesian methods to model manatee abundance from aerial survey data while accounting for spatial heterogeneity in detection and abundance. We then applied the collision risk methodology to predict expected relative mortality risk in space and time for several speed zone scenarios and used this metric in a decision analysis framework to determine optimal protection zones.

2 | MATERIALS AND METHODS

2.1 | Study area and data

Our study area covered a portion of Collier County, Florida (Supporting Information Figure S1-1). GIS data that we used included:

aerial survey sightings for manatees and boats, shoreline, seagrass distribution, urban development, and watercraft channels (Bauduin et al., 2013; see Supporting Information Appendix S1 for a detailed description of data sources). To estimate manatee abundance, we used manatee counts and flight paths from eight GPS-tracked, single-pass, aerial surveys spanning July 2007 to May 2008 (Bauduin et al., 2013). To estimate boat abundance, we used boat counts from 11 aerial surveys conducted between December 2006 and November 2007 (Gorzelany, 2008). Surveys were classified into seasonal categories based on survey date and patterns in the raw counts corresponding to: (a) a hot "summer" season (June–August), (b) a warm "spring/fall" season (March–May and September–October), (c) a cool "winter" season (November–December and February), and (d) a cold "mid-winter" season (January) (see Supporting Information Appendix S2: Figure S2-1 for more details). For the manatee and boat parameters in the collision risk framework, we used previously published estimates (Edwards et al., 2016 for the probability that manatees are within strike depth; Martin et al., 2016 for all others).

For the manatee and boat abundance analyses, we used a sampling grid ($n = 289$, grid cell size = 1 km²) and designated the water portion in each grid cell as the sampling unit (we refer to each grid cell as a site). For the collision risk analyses, we considered the channel and nonchannel portions of each site as separate management units ($n = 389$ sites) (see Supporting Information Appendix S1).

We additionally provide the R codes, JAGS codes, and data needed to conduct all analyses in this work (Udell et al., 2018).

2.2 | Abundance estimation

We modelled manatee abundance (N) from aerial survey counts using a Poisson-hurdle variant of an N-mixture model (Dorazio, Martin, & Edwards, 2013), which accounts for rarity by simultaneously modelling occupancy (ψ), mean abundance given occupancy (λ), and detection (p). Abundance has an expected value of $N = \lambda \times \phi$, where $\phi = \frac{\psi}{(1-e^{-\lambda})}$ (Johnson, Kemp, & Kotz, 2005). Dorazio et al. (2013) used a maximum likelihood approach, whereas we analysed this model with a Bayesian approach. The model formulation that we used is as follows:

$$z_{i,j} \sim \text{Bernoulli}(\psi_{i,j}) \tag{1}$$

$$N_{i,j} \sim \begin{cases} 0 & \text{if } z_{i,j} = 0 \\ \text{TrPois}(\lambda_{i,j}) & \text{if } z_{i,j} = 1 \end{cases} \tag{2}$$

$$P(N_{i,j} = k_{i,j} | N_{i,j} \geq 0) = \frac{e^{-\lambda_{i,j}} \lambda_{i,j}^{k_{i,j}}}{k_{i,j}! (1 - e^{-\lambda_{i,j}})} \tag{3}$$

where i is an index for each site (sampling unit), and j is an index for each survey. The latent occupancy status $z_{i,j}$ ($z_{i,j} = 1$ if the site is occupied and 0 otherwise) is distributed according to a Bernoulli distribution with parameter $\psi_{i,j}$ (Equation 1). If the site is unoccupied ($z_{i,j} = 0$), then $N_{i,j} = 0$, otherwise $N_{i,j}$ follows a zero-truncated Poisson (TrPois) distribution (Equation 2) with a probability mass function described in Equation 3 (Dorazio et al., 2013).

The parameters of the hurdle abundance model can be estimated with an N-mixture approach to account for imperfect detection of manatees (Dorazio et al., 2013). N-mixture models typically use repeated surveys to estimate detection. Our surveys were single-pass (not repeated), and we instead used Bayesian analysis and ancillary studies (Martin et al., 2015) to inform the detection process. Using informative priors (see Supporting Information Appendix S2) and geo-tracked flight paths allowed us to estimate abundance for single-pass surveys without incurring identifiability issues. The observation model is described in Equations 4–8:

$$C_{i,j} \sim \text{Binomial}(N_{i,j}, p_{(t)_{i,j}}) \tag{4}$$

$$p_{(t)_{i,j}} = p_{(a)_{i,j}} \times p_{(p)_{i,j}} \tag{5}$$

$$p_{(p)_{i,j}} \sim \text{Beta}(a_1, b_1) \tag{6}$$

$$p_{(a)_{i,j}} = \sum_{vk=2,3,4} \sum_{dist=1,2,3} w_{vk,dist,i,j} \times \text{rbeta}_{vk,dist,i,j}^{\text{threshold}} \tag{7}$$

$$\text{rbeta}_{vk,dist,i,j}^{\text{threshold}} \sim \text{Beta}(a_{2,vk,dist}, b_{2,vk,dist}) \tag{8}$$

Manatee counts ($C_{i,j}$) at site i and survey j follow a binomial distribution with the parameters: abundance ($N_{i,j}$) and total detection probability ($p_{(t)_{i,j}}$) for each site and survey (Equation 4). The total detection probability is the product of the probability of availability ($p_{(a)_{i,j}}$) and the probability of perception given availability ($p_{(p)_{i,j}}$) (Equation 5). The latter term was quantified for the primary observer in a previous study (Martin et al., 2015) and was modelled using a beta distribution as an informative prior (Equation 6). We define $p_{(a)_{i,j}}$ as the weighted average of the probability a manatee is above a critical depth threshold ($\text{rbeta}_{vk,dist,i,j}^{\text{threshold}}$) (Equation 7) necessary to be detectable in each of three visibility/turbidity (vk) and three distance (dist) categories (Equation 8). The weights ($w_{vk,dist,i,j}$) correspond to the proportion of sampled area in each distance and visibility class for each site and survey (Martin et al., 2015; see Supporting Information Appendix S2).

Manatee occupancy ($\psi_{m_{i,j}}$) and abundance given occupancy ($\lambda_{m_{i,j}}$) were modelled for each site with categorical fixed effects of region and season, and continuous fixed effects of distance to seagrass and distance to development (see Supporting Information Appendix S2). For the estimation process, the proportion of area sampled within each cell during each survey was included as a continuous covariate for $\lambda_{m_{i,j}}$. After estimating the coefficients of the area covariate for each season, we used these coefficients to make abundance predictions for the entire area of each cell (including the nonsampled portions) for each season. We treated area as a covariate rather than a log-offset, as it greatly improved model convergence.

Boat abundance was modelled with a similar approach, although the detection of boats was assumed to be perfect (Bauduin et al., 2013; Supporting Information Appendix S2). Thus, we used a hurdle model (Equations 1–3), but unlike the manatee model, we assumed that occupancy and abundance were observed. Boats were counted from videos collected during aerial surveys which reduced the potential for counting errors. Occupancy ($\psi_{b_{i,j}}$) and abundance given

occupancy ($\lambda_{b_{i,j}}$) for each site and survey were modelled as a function of the following covariates: region, season, distance to shore, length of channel, time of day (PM vs. AM), and day of week (weekend vs. weekday) (see Supporting Information Appendix S2). Total water area in each site surveyed was also included as a covariate for λ_{b_i}. We accounted for over-dispersion in boat abundance with the use of site-level random effects which, along with their corresponding precision parameters, varied by region and season (Kéry & Schaub, 2012). We estimated the parameters' posterior distributions using Markov chain Monte Carlo (MCMC) with JAGS 4.2.0 (Plummer, 2015) and the package RJAGS (Plummer, 2016) in program R version 3.3 (R Core Team, 2016) (see Supporting Information Appendix S2 for more details).

We used these models to predict the expected values of manatee abundance and boat abundance for each site and season. For boats, we also weighted the predictions for each season with respect to the time of day (AM vs. PM) and day of week (weekday vs. weekend) effects (e.g., a weight of $\left(\frac{1}{2} \times \frac{2}{7}\right)$ for AM and weekend predictions). We also calculated an annual weighted average in each site for manatees and watercraft based on their respective seasonal predictions and the number of days in each season (Supporting Information Figure S2-1). Standard errors and 95% credible intervals (CRI) for predicted abundance were obtained by using MCMC samples of lower level parameters.

2.3 | Collision risk

We evaluated the relative risk of deadly collisions across the study area under several scenarios that varied in timeframe of abundance predictions (year mean and seasonal), management zones (current speed zones vs. no-protection), and in the relationship between probability of death given strike speed (Pr(*death|speed*)) (Supporting Information Figure S3-1). The current speed zones in the study area are designated in miles per hour (mph) and include unregulated (we assume 30 mph [48.28 km/h]), 20 mph (32.19 km/h), 7 mph/slow (11.27 km/h), and 3 mph/idle (4.83 km/h) zones, with speed regulations typically differing inside and outside of channels.

The analytical encounter rate framework is built on principles similar to ideal gas models (Hutchinson & Waser, 2007) and takes into account the area of interaction and the sizes, speeds, and abundances of mobile agents (Gerritsen & Strickler, 1977; Gurarie & Ovaskainen, 2013; Martin et al., 2016). The stochastic form for the encounter process (a Poisson process) is derived by assuming that the times until first encounter are distributed exponentially (Martin et al., 2016). We first applied this analytical equation to each site (*i*) and for each scenario (defined in the previous paragraph). The encounter rate γ_i (for a single manatee and a single boat) is a function of manatee and boat speeds [$I(v_m, v_b)f_v(v_m)$] (see appendix S1 in Martin et al., 2016), sizes ($r_c = r_m + r_b$), and the surface area of encounter (S_i) (Equation 9) and can be written as (Martin et al., 2016):

$$\gamma_i = \frac{2 r_c}{S_i} \int_{v_m} I(v_m, v_b) f_v(v_m) d v_m \tag{9}$$

where v_m is the velocity of manatees, v_b is the velocity of boats, r_m is the radius of manatee size, r_b is the radius of boat size, and r_c is the critical radius of encounter based on r_m and r_b (see Supporting Information Table S3-1 for list of parameters). Function I is a monotonic function of manatee and boat speeds:

$$I(v_m, v_b) = \int_0^{2\pi} \sqrt{v_m^2 + v_b^2 - 2v_m v_b cos(\theta)} \frac{d\theta}{2\pi} \tag{10}$$

and $f_v(v_m)$ is the probability distribution of animal velocity (Weibull distribution with shape = 0.72, scale = 0.16; M = 0.20 m/s, SD = 0.28; Martin et al., 2016; Supporting Information Appendix S3).

We used a "fixed distance" scenario (the distance travelled by boats is constant regardless of speed regulation) to model collisions, described in Martin et al. (2016). With this formulation, $\left(\frac{distance_i}{speed_i}\right)$ is equivalent to time in seconds per boat transit for each site *i*. Data on boat transit distances were not available for this study; thus, we estimated the expected distance as a function of site size (Kuchel & Vaughan, 1981; Supporting Information Appendix S3). The encounter rate for a site γ_i^* was scaled according to the expected number of boats ($E[N_b]_i$), number of manatees ($E[N_m]_i$) and the number of transits per day ($N_{transit}$) across a given timeframe (N_{days}) of interest (Equation 11) as follows:

$$\gamma_i^* = \gamma_i E[N_b]_i E[N_m]_i \left(\frac{distance_i}{speed_i}\right) N_{transit} N_{days} \tag{11}$$

Next, we used Monte Carlo simulations to account for probabilistic interactions, such as the probability a manatee was within strike depth given presence of seagrass Pr(strike|seagrass$_i$) and Pr(death|speed) (Supporting Information Appendix S3). The number of encounters at each site ($N_{encounters_i}$) was modelled as a Poisson process, with a rate parameter (γ_i^*) (Equation 12):

$$N_{encounters_i} \sim Poisson(\gamma_i^*) \tag{12}$$

The number of impacts (N_{impact_i}) follows a binomial distribution based on the number of encounters ($N_{encounters_i}$) and Pr(strike|seagrass$_i$). The Pr(strike|seagrass$_i$) for each site varies based on presence of seagrass and follows a beta distribution with parameters estimated from manatees in a previous study (Edwards et al., 2016, Supporting Information Appendix S3):

$$N_{impact_i} \sim Binomial\left(N_{encounters_i}, Pr(strike|seagrass_i)\right) \tag{13}$$

As probabilities of behavioural avoidance and death given boat speed are unknown, we set avoidance probability to zero, and investigated different linear relationships for Pr(death|speed). We named the various putative relationships for Pr(death|speed) for the speed in mph at which Pr(death) = 1 (mortality model M*x* corresponds to Pr(death) = 1 at *x* mph; for example, M13 corresponds to Pr(death) = 1 at 13 mph) (Supporting Information Appendix S3: Figure S3-1). The number of deaths (N_{deaths_i}) at each site follows a binomial distribution given the expected number of impacts at each site (N_{impact_i}) and Pr(death|speed$_i$):

$$N_{deaths_i} \sim Binomial(N_{impact_i}, Pr(death|speed_i)) \tag{14}$$

We evaluated the effectiveness of the current protection zones for each of the Pr(death|speed) relationships by comparing their relative risk (and 95% credible intervals) to a no-protection scenario (boat speed: 30 mph). We calculated the total and percent relative risk reduction (and 95% credible intervals) that the current management zones provide relative to no-protection, as well as a test statistic, Pr(Change > 0), as the proportion of Monte Carlo samples where the difference in relative risk is greater than zero.

2.4 | Optimizing protection zones

To determine the optimal configuration of speed zones, we first specified two alternative management objectives: (a) minimize regulatory burden on boaters (hereafter referred as cost) while maintaining relative risk at or less than current levels ("MinCost" scenario), and (b) minimize relative risk while maintaining cost at or below current levels ("MinRisk" scenario). We developed a cost index for each site to reflect the regulatory burden on waterway users. This index was based on the amount of regulated area, the expected watercraft abundance, and on speed regulations (Supporting Information Appendix S4). We calculated a base cost as a function of area and expected watercraft abundance at each site. Area of a site is often used as a proxy for cost in conservation planning (Moilanen et al., 2009) and in this example more area regulated reflects higher costs to waterway users. We added an additional cost for expected watercraft abundance to reflect the number of users impacted. Base cost was increased 3-fold for sites containing channels (which ensured that speeds in channels were greater or equal to speeds outside of channels). Finally, we applied a zone multiplier to the base cost in each site (determined as $\frac{1}{\text{speed}}$ to reflect differences in travel time), so that the base cost scaled meaningfully with the level of regulatory burden.

2.4.1 | Decision Analysis and Linear Integer Programming

We considered sites $i \in \{1, \ldots, n\}$ where watercraft speed may be regulated below 30 mph or, in the absence of regulation, speed was assumed to be 30 mph. We assigned a speed class to each site i, denoted $v_i = 1, 2, 3, 4$, corresponding to 30, 20, 7, and 3 mph. Imposing a speed regulation v_i on site i produces a risk ($r_{v_i}^i$) and a cost ($c_{v_i}^i$). A regulation rule, δ, is a set of speed zones for the study area and the optimization problem consists of computing the optimal set of speed zones, δ^*, which minimizes the objective function with respect to a set of constraints.

We propose the following encoding of this problem using a Linear Integer Programming (LIP) approach. A regulation δ is fully defined by the speed classes in each site. Because we have four possible speeds in each site, the control vector x_δ is a vector of zeros and ones of length $4 \times n$. x_δ encodes the speed in each site as follows: if index k in vector x_δ, $x_\delta(k)$, equals 1, then the speed in site i (where $i = \text{floor}\left(\frac{k}{5}\right) + 1$) is equal to $\text{mod}(k, 4) + 4 \times 1_{\{\text{mod}(k,4)\}}$. The floor function rounds down to the nearest integer, mod is the modulus (or remainder) after division and $1_{\{\text{mod}(k,4)\}}$ equals 1 when $\text{mod}(k, 4) = 0$ and 0 otherwise. For example, for two sites ($n = 2$), $x_\delta = (0, 1, 0, 0, 0, 0, 0, 1)$ corresponds to regulation δ where the first site has speed "2" (20 mph) and the second site has speed "4" (3 mph). We used the same principle to define the risk and cost vectors r and c, respectively. For example, again when $n = 2$, we have $r = \left(r_1^1, r_2^1, r_3^1, r_4^1, r_1^2, r_2^2, r_3^2, r_4^2\right)$. Depending on the management objective, the value of a regulation rule is either the total risk, $\text{Risk}(\delta) = \sum_{i=1}^n r_{v_i} = x_\delta^T \times r$, or the total cost, $\text{Cost}(\delta) = \sum_{i=1}^n c_{v_i} = x_\delta^T \times c$.

We define two separate management problems for the optimization. The first problem, referred to as the Minimize-Cost (MinCost) scenario, has the objective of minimizing the total cost of management while maintaining total risk at or below the current risk (Equation 15):

$$\text{MinCost Scenario:} \begin{cases} \delta^* = \arg\min x_\delta^T \times c, \\ \text{such that } x_\delta^T \times r \le R_{\text{current}} \\ A \times x_\delta^T = O \end{cases} \quad (15)$$

The second, referred to as the Minimize-Risk (MinRisk) scenario, has the objective to minimize the total expected risk while maintaining the total cost at or below the current cost (Equation 16):

$$\text{MinRisk Scenario:} \begin{cases} \delta^* = \arg\min x_\delta^T \times r, \\ \text{such that } x_\delta^T \times c \le C_{\text{current}} \\ A \times x_\delta^T = O \end{cases} \quad (16)$$

R_{current} is the current risk and C_{current} is the current cost. $A \times x_\delta^T = O$ represents a set of constraints ensuring the problem is properly defined (only one speed zone can be selected per site; Supporting Information Appendix S4).

We solved these optimization problems using LIP (Nocedal & Wright, 2006) for each abundance (*year mean* and *seasonal*) scenario and mortality–speed relationship for the collision analysis. We used package lpSolve in program R to determine the optimal solutions under these constraints, using the branch and bound method (Berkelaar, 2015). We evaluated the effectiveness of the optimal protection zones by comparing their total cost and relative risk to: (a) no-protection and (b) the current management zones.

2.4.2 | Spatial aggregation of zones and the Pareto efficient frontier

Aggregating protection zones in space can be a secondary objective of managers to reduce cost and improve compliance. We address this problem by postprocessing the LIP solutions to improve the spatial aggregation of protection zones. We then compare these zones in terms of relative risk and cost to the Pareto efficient frontier. In our case, the Pareto efficient frontier represents the maximum possible risk reduction (solved from the LIP zones) across the entire range of possible costs. This frontier may also serve as a benchmark for comparing zones that consider additional logistical constraints and *ad hoc* adjustments by managers.
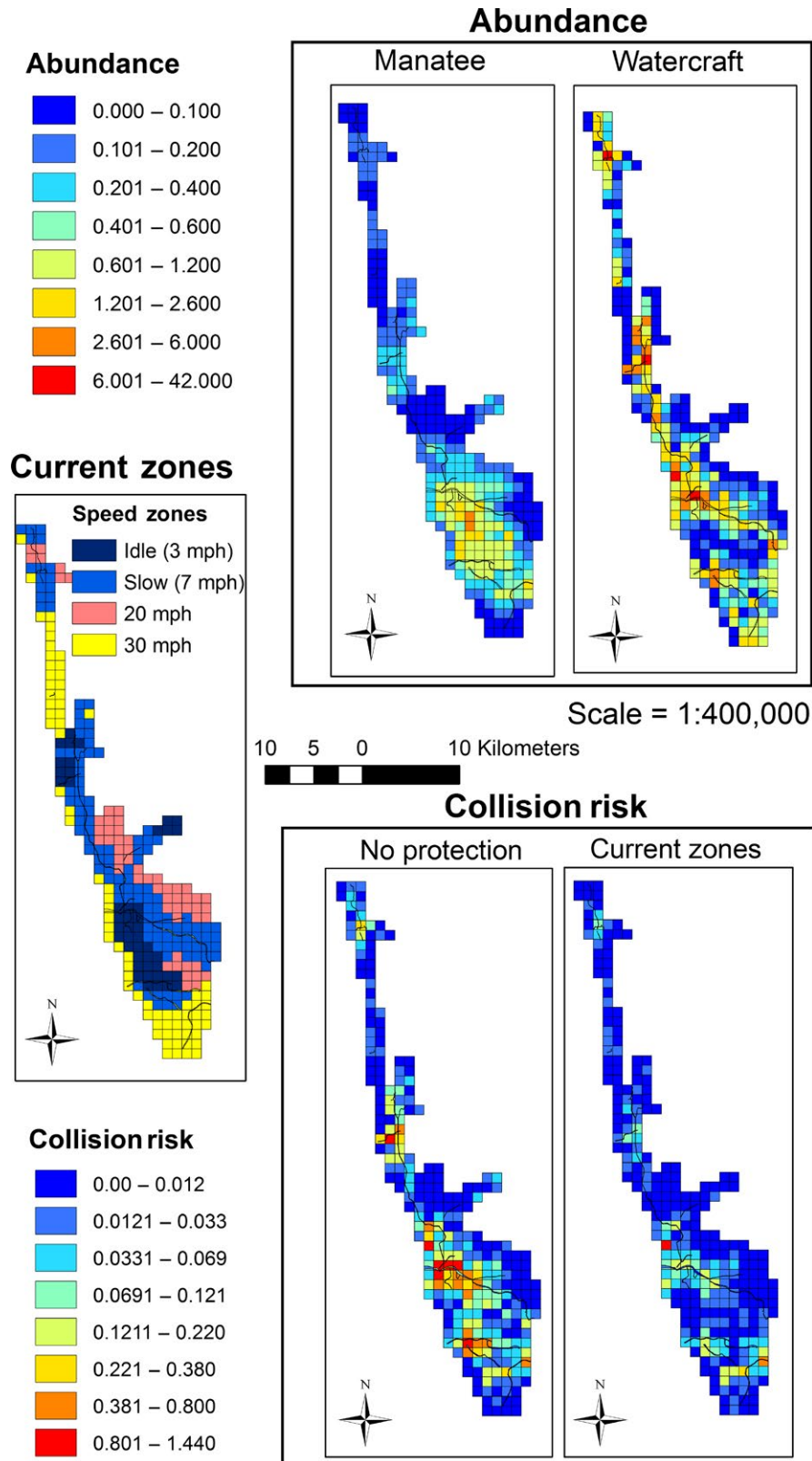
FIGURE 1 Top panel: Map of the weighted year mean abundance predictions of manatees (left) and boats (right) in the study area. Left-middle panel: The current speed zones are depicted by showing the speed limits in each cell. Bottom panel: Map of risk in the study area under no-protection (left panel) vs. risk under current management (right panel) for the weighted year means for manatee and boat abundance. Model M200 was considered for the probability of death given strike speed (Supporting Information Appendix S3); units are relative number of manatee deaths. Note the 30 mph zones correspond to unregulated sites
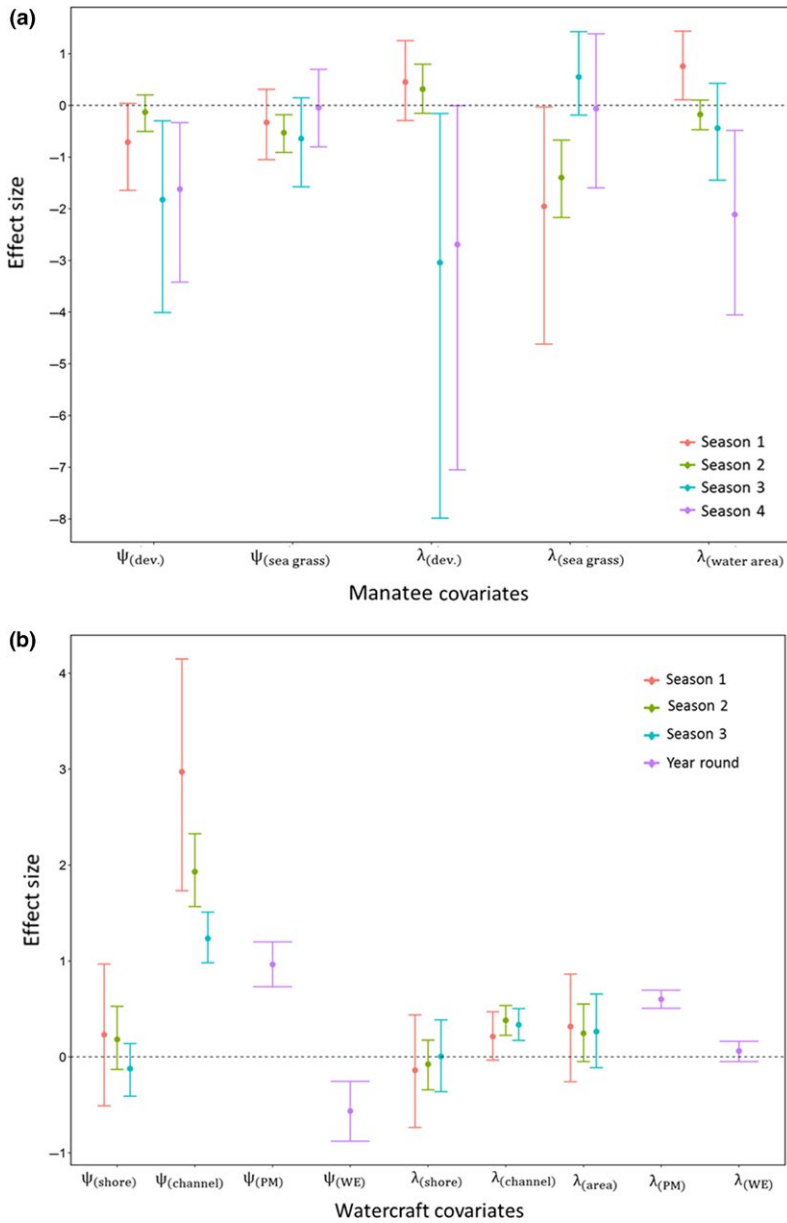
FIGURE 2 Point estimates and 95% CRIs for covariate effect sizes on occupancy (ψ) and abundance given occupancy (λ) for manatees (a) and watercraft (b). See Supporting information Equations S2-1 to S2-4 for more details. "Sea grass" and "dev" represent distance to sea grass and development, respectively. For watercraft, "channel" represents length of channel in each site, "shore" represents distance to shore, and PM and WE represent evening and weekend effects, respectively

We developed a postprocessing algorithm to improve the compactness of the LIP zones and we generated zone alternatives to compare to the Pareto frontier. This algorithm uses two possible strategies; one is risk-averse and the other is cost-averse (see Supporting Information Appendix S5 for details). For example, the risk-averse strategy starts with the strictest zones (3 mph) and converts neighbours above a certain base risk quantile (q1) to 3 mph. This process was then repeated for 7 mph zones, using a lower threshold for risk (q2), and again for the 20 mph zones using a third threshold (q3). In contrast, the cost-averse strategy starts with the least costly zones (30 mph) and uses cost rather than risk thresholds. Both strategies have the option to use a majority filter after initial smoothing to convert sites without a single common neighbour to the most common zone among its neighbours. The performance of zones using additional smoothing options was investigated in Supporting Information Appendix S5. Based on visual inspection

of the zones, we found that the values of q1 = 0.8, q2 = 0.7, and q3 = 0.6 led to improved spatial aggregation.

3 | RESULTS

3.1 | Abundance

Predicted manatee abundance in the study area was highest in the summer and lowest in the cold season (Supporting Information Table S2-2 and Figure S2-2). For the weighted year mean, manatee abundance was concentrated in the southern portion of the study area (Figure 1). Manatees were more dispersed during Seasons 1 and 2, and more clustered around the Marco Island canal system during the winter seasons (3 and 4) (Supporting Information Figure S2-2). The covariate effects on manatee occupancy and abundance given occupancy (ψ_m and λ_m) varied seasonally in direction and significance (CRIs

did not overlap zero) (Figure 2, Supporting Information Appendix S2: Table S2-4, for further results see).

Watercraft abundance varied across seasons, with the highest numbers generally occurring in the spring/fall periods and the lowest during the winter season (Supporting Information Table S2-2 and Figure S2-2). Distribution was relatively consistent across seasons (Supporting Information Figure S2-2). Not surprisingly, watercraft was concentrated in sites with channels (Figures 1 and Supporting Information Figure S1-1), and the length of channel in each plot was consistently the strongest predictor of watercraft occupancy and abundance (Figure 2, Supporting Information Table S2-5).

3.2 | Relative lethal collision risk

The expected effectiveness of the current zones compared to no-protection was visualized by mapping relative lethal risk in each site under both management scenarios (Figure 1). The expected reduction in total relative deaths compared to no-protection was significantly greater than zero for all mortality–speed relationships considered (Figure 3). Percent relative risk reduction (Supporting Information Figure S4-1) also indicated a significant reduction in annual relative risk (Table 1). On an annual timeframe, relative risk under the current zones averaged 51.5%–70.0% lower than risk under the no-protection scenario (Table 1, Supporting Information

Figure S4-1). Additionally, $\Pr(\text{Change} > 0)$ was equal to 1.0 for all year-abundance scenarios and was above 0.95 for all but four of the seasonal abundance and $\Pr(\text{death}|\text{speed})$ combinations (Table 1). Relative risk varied with season (Supporting Information Table S3-2), generally tracking the change in seasonal abundance of manatees and boats (Supporting Information Table S2-2).

3.3 | Optimal allocation of protection zones

The optimal minimum cost (MinCost) and minimum risk (MinRisk) zone configurations for the annual mean abundances are presented in Figure 4 for each relationship of $\Pr(\text{death}|\text{speed})$. The MinRisk zones significantly reduced the annual relative risk compared to the no-protection scenario and also reduced relative risk compared to the current zones, all for the same cost as the current zones (Figure 3, Supporting Information Figure S4-1). The MinCost zones significantly reduced relative risk compared to the no-protection scenario and had near identical relative risk as current zones (Figure 3, Supporting Information Figure S4-1).

The Pareto efficient frontier illustrates that potential risk reduction is an increasing and saturating function of cost (Figure 5). The MinCost zones and MinRisk zones lie directly on this curve and had the same relative risk and cost, respectively, as the current zones. Some of the MinCost zones spatially smoothed with a risk-averse
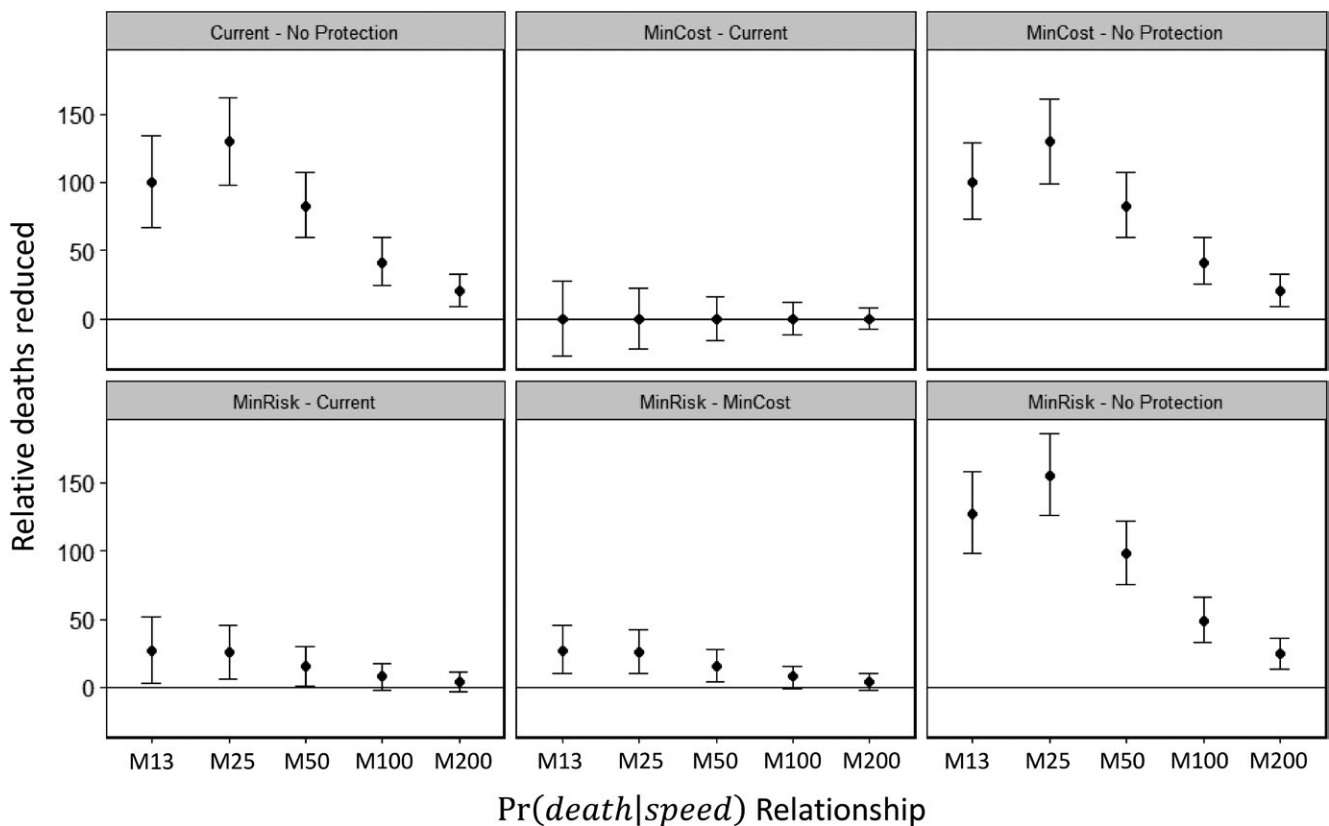

FIGURE 3 Posterior means and 95% CRIs of total reduction in relative deaths under different zone comparisons (current protection zones, no-protection, and optimal configurations for MinCost and MinRisk) for each model for $\Pr(\text{death}|\text{speed})$ (M13–M200), using the weighted year means for manatee and boat abundance

Abundance	Pr(death|speed)	% RRR Mean	RRR 95% CRI	Pr(Change > 0)
Year	M13	51.5	(38.8–62.7)	1.000
Year	M25	66.8	(56.7–75.6)	1.000
Year	M50	70.0	(57.6–80.4)	1.000
Year	M100	69.7	(51.1–84.1)	1.000
Year	M200	69.1	(40.9–88.9)	1.000
S1	M13	50.8	(25.9–70.1)	0.999
S1	M25	65.0	(44.9–80.6)	1.000
S1	M50	67.5	(41.9–86.1)	1.000
S1	M100	66.6	(25.0–91.7)	0.994
S1	M200	63.8	(0.0–100)	0.957
S2	M13	48.7	(29.9–64.2)	1.000
S2	M25	63.8	(48.8–76.2)	1.000
S2	M50	68.8	(48.1–81.6)	1.000
S2	M100	66.2	(37.5–86.5)	0.999
S2	M200	64.9	(18.2–92.9)	0.989
S3	M13	59.9	(10.0–90.0)	0.982
S3	M25	77.3	(42.9–100.0)	0.998
S3	M50	79.7	(33.0–100.0)	0.991
S3	M100	76.5	(0.0–100.0)	0.942
S3	M200	75.2	(0.0–100.0)	0.866
S4	M13	55.5	(0.0–90.0)	0.96
S4	M25	74.2	(33.3–100.0)	0.995
S4	M50	76.6	(20.0–100.0)	0.98
S4	M100	73.2	(0.0–100.0)	0.913
S4	M200	72.7	(0.0–100.0)	0.834

TABLE 1 Percent relative risk reductions for manatees (RRR) (means and 95% credible intervals) between no-protection and the current zones, and the probability that relative risk reduction is greater than zero (Pr(Change > 0)) for each abundance and mortality model (M13 to M200). Estimates are presented for each season (S1–S4) and for year average (year)

strategy and MinRisk zones spatially smoothed with a cost-averse strategy (Figure 5 and Supporting Information Figure S5-2) fell near the Pareto frontier and were therefore near optimal.

4 | DISCUSSION

By combining two paradigms—encounter rate theory and decision analysis—we have formalized a framework for linking management actions to ecological interactions (e.g., collision process) for the purpose of evaluating and optimizing management decisions. Managers can use this approach to evaluate and to improve upon the effectiveness of actions, such as in the design of protection zones for wildlife. The decision analysis component helps prioritize management actions by considering the total relative risk and socioeconomic costs of those actions. We demonstrated the application of this approach by using it to evaluate and optimize the design of speed zones established to protect the imperiled Florida manatee.
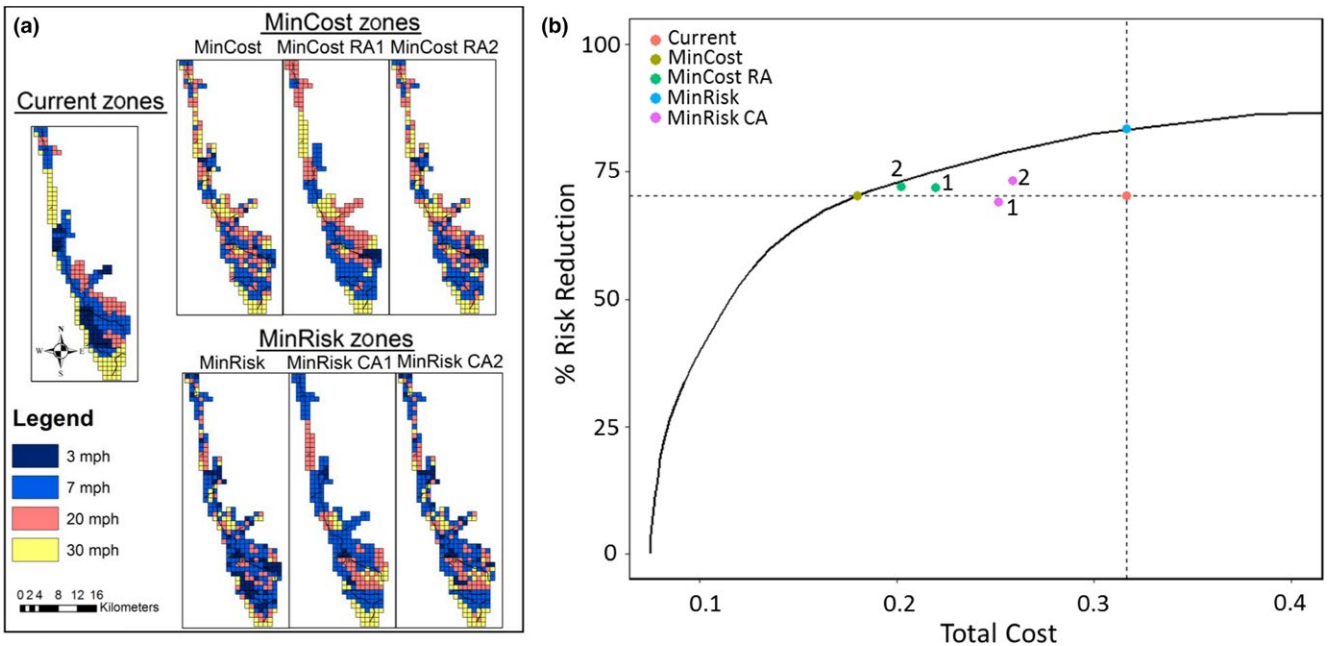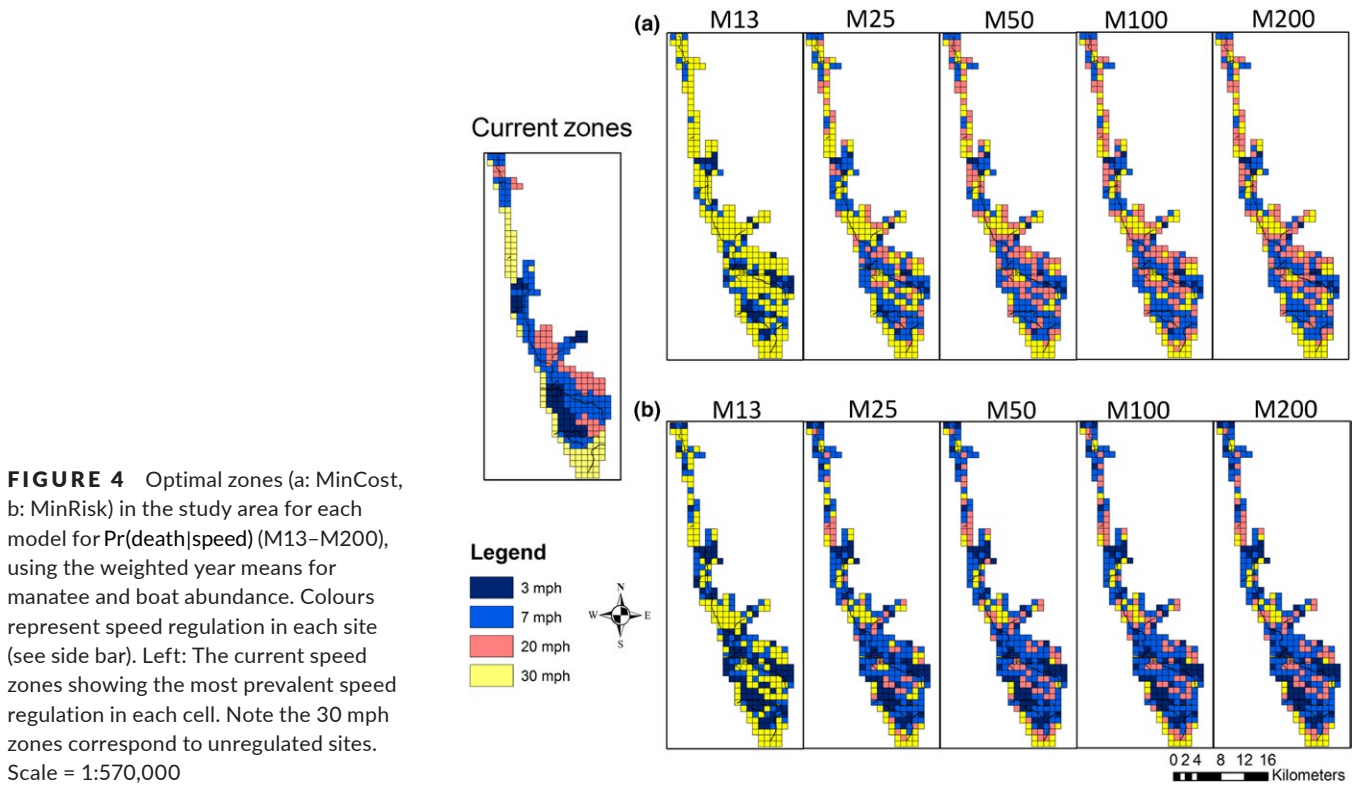
4.1 | Manatee and boat abundance

Abundances of manatees and boats were important in influencing the relative lethal collision risk to manatees, the cost to boaters, and

the optimal configuration of protection zones. To our knowledge, this is the first time abundance predictions (modelled in space and time, and accounting for imperfect detection) have been used to evaluate the risk of collision to wildlife and to optimize boat speed regulations. We implemented a hurdle N-mixture model with a detection model based on manatee availability and human perception bias that accounted for manatee distance from the observer, spatial heterogeneity in water turbidity, and manatee diving behaviour. Modifying the framework of Martin et al. (2015) with a hurdle approach allowed us to estimate and predict manatee occupancy and abundance given occupancy in each site using the same continuous spatial covariates (e.g., distance to seagrass) without incurring identifiability issues (Dorazio et al., 2013). Our analyses showed that abundance and distribution of manatees varied substantially across seasons (Supporting Information Table S2-2 and Figure S2-2). This was not surprising, given constraints on manatee habitat selection during cold months, when manatees have thermal limitations on resource use (Haase, Fletcher, Slone, Reid, & Butler, 2017).

4.2 | Collision risk

Our methodology allowed us to estimate the relative risk of mortality, because absolute risk cannot be estimated without information

FIGURE 4 Optimal zones (a: MinCost, b: MinRisk) in the study area for each model for Pr(death|speed) (M13–M200), using the weighted year means for manatee and boat abundance. Colours represent speed regulation in each site (see side bar). Left: The current speed zones showing the most prevalent speed regulation in each cell. Note the 30 mph zones correspond to unregulated sites. Scale = 1:570,000

FIGURE 5 (a) MinCost zones spatially smoothed according to risk-averse strategies (RA) and MinRisk zones spatially smoothed according to cost-averse strategies (CA). (b) Pareto frontier, representing the percent risk reduction provided by optimal zones (compared to no-protection) given cost, and the performance of the smoothed zone alternatives using the M200 Pr(death|speed) mortality model. The vertical dashed line indicates cost for the MinRisk and current configurations; the horizontal dashed line indicates risk reduction for the MinCost and current configurations. Configuration alternatives for a and b include MinCost zones smoothed according to a risk-averse (RA) strategy and MinRisk zones smoothed according to a cost-averse (CA) strategy, with labels indicating which of two options were used for the spatial smoothing algorithm (1: with a majority filter and 2: without a majority filter) (see Supporting Information Appendix S5 for more details)

about the probability of avoidance and the Pr(death|speed) (see appendix S4 in Martin et al., 2016). We therefore examined alternative, hypothetical models to explore the influence of Pr(death|speed) on

relative risk while assuming an avoidance probability of zero. While we did not include avoidance probability in this analysis, this parameter can be incorporated in future analyses once estimated (Martin

et al., 2016). Our analyses emphasize the importance of estimating the probability of death given strike speed (Figure 3), although this is a difficult relationship to quantify (Conn & Silber, 2013; Vanderlaan & Taggart, 2007). As more information accumulates, the risk model can be refined. Nevertheless, one metric we selected to compare scenarios—mean percent relative risk reduction—appears to be consistent across mortality models (Table 1, Supporting Information Figure S4-1).

For most management applications, a relative risk metric may be sufficient for evaluating and optimizing the efficiency of speed zones. The current analyses provide useful insights for management and suggest the current speed zones in the study area are effective in reducing relative lethal collision risk to manatees under the mortality relationships considered (Figure 3, Table 1). Objectively quantifying the effectiveness of speed zones has presented a difficult challenge (Calleson, 2014; Laist & Shaw, 2006), so we believe that our work represents a significant leap forward. Effectiveness would be reduced with less than full compliance by boaters, or if average boat speeds were less than 30 mph when unregulated. Future analyses could also incorporate an empirical distribution of boat speed in unregulated areas.

4.3 | Spatial optimization of protection zones

An innovative aspect of our framework is that we used encounter rate theory to explicitly prioritize interactions (i.e., lethal collisions) between moving agents when designing management zones. This allowed us to quantify and optimize the effectiveness of management actions in terms of relative lethal collision risk rather than using a proxy such as co-occupancy. The optimal MinCost zones, like the current configuration of zones, significantly reduce relative risk compared to the no-protection case for all Pr(death|speed) models considered, and the MinRisk zones reduced relative risk even further (Figure 3).

The optimal zones for both objective functions were similar across Pr(death|speed) relationships, except for one that seems unrealistic in which death is certain in collisions where the boat is travelling at least 13 mph (M13, Figure 4). The similarity of the optimal zones may seem counterintuitive because the total amount of risk in the study area is lessened as the relationship between speed and mortality weakens. The similarity in zones arises because we used a relative risk metric, dependent on the assumed linear relationships for Pr(death|speed), as the objective function in the MinRisk solutions and as a constraint in the MinCost solutions. The difference in optimal zones under the M13 relationship compared to the others arises because the relative risk is equivalent between the 20 and 30 mph zones (both have a Pr(death|speed) of 1), yet the cost is higher for the 20 mph zones.

While we modelled seasonal abundance and relative collision risk, we did not consider seasonal zones for the decision analysis because there are currently year-round protection zones in the study area. Although, it is possible that seasonal zones could increase efficiency, enforcing seasonal zones is currently impractical. The output

from the optimization algorithm can be used as a decision-support tool for managers designing effective speed zones. It should not be interpreted as a prescription, however, because managers may have additional objectives, data sources, and constraints to consider. We created an algorithm for improving the spatial aggregation of the LIP zones based on risk-averse or cost-averse strategies. We introduced the concept of the Pareto frontier as a means of evaluating these and other alternative zone configurations that impose additional considerations (e.g., greater spatial aggregation). Some of the smoothed zones are more efficient than the current zones in terms of both risk and cost (Figure 5: points fall above the horizontal line and left of the vertical line). Also, some of these zones, as well as some of the zones with additional smoothing options (Supporting Information Figure S5-2), lie very close to the Pareto frontier indicating that they are near optimal while providing improved levels of spatial aggregation.

Quantifying the "true" socioeconomic cost of speed regulations was beyond the scope of this study. Future developments should consider refining the objective function to better reflect the values of stakeholders and the cost of enforcement. This may be achieved with the use of formal elicitation techniques (Goodwin & Wright, 2009). An extension of this work might also consider scenarios in which the establishment of speed zones not only affects boat speed, but also changes the distribution of boats as vessel operators shift to less regulated areas.

Our framework can be applied to other conservation planning efforts which focus on wildlife interactions, such as optimal placement of wind turbines to reduce bat mortality and spatial fishing closures to reduce risk of bycatch. In fact, this general framework could be applied to most problems of human–wildlife conflict where the interaction rate (e.g., poaching, invasive removal) is of management interest. Prerequisite data to determine analytical encounter rates include information about densities, sizes and speeds of the interacting agents, and the area of interaction. Additional data and analysis (e.g., telemetry and video studies) would be needed to quantify probabilistic interactions that occur given a deterministic encounter and the effects of management on these relationships. Management actions could influence any of the variables in the encounter rate framework, and if trade-offs in the outcomes of management actions can be identified between the interaction rate and cost of management, our decision analysis framework could be used to identify optimal actions.

5 | CONCLUSIONS

We have presented a framework that explicitly links management actions to relative lethal encounter risk, and this risk can be used as a metric in formal conservation planning. We used the example of collision risk between Florida manatees and watercraft, one of many relevant issues that may be framed through encounter rate theory, to demonstrate how such a framework can be applied. Not only can this methodology be used to evaluate the effectiveness of current or proposed management actions in reducing relative risk, it can also

be used to optimize protection zones. We determined optimal solutions which either minimized the relative risk to manatees given the current management costs, or minimized the cost to waterway users given the risk under current management. In addition, we devised a simple method for improving the spatial aggregation of the optimal zones and used the concept of the Pareto efficient frontier as a benchmark for comparing alternative zone configurations. This general framework could be applied to modelling and optimizing the management of many wildlife–human conflicts where an interaction rate is of direct management interest.

ACKNOWLEDGEMENTS

AUTHORS' CONTRIBUTIONS

B.J.U., J.M., R.J.F., T.A.G., E.G., C.S.C. conceived the ideas, B.J.U., J.M., R.J.F., M.B., T. AG., H.H.E., S.K.H. contributed to the analysis. All authors contributed to writing and approved the final version for publication.

DATA ACCESSIBILITY

Data and code used for the analysis are available at the Dryad Digital Repository https://doi.org/10.5061/dryad.7dh4312 (Udell et al., 2018).

ORCID

Bradley J. Udell http://orcid.org/0000-0001-5225-4959

Julien Martin http://orcid.org/0000-0002-7375-129X

Robert J. Fletcher http://orcid.org/0000-0003-1717-5707

Mathieu Bonneau http://orcid.org/0000-0002-7004-8267

Eliezer Gurarie http://orcid.org/0000-0002-8666-9674

REFERENCES

Aipanjiguly, S., Jacobson, S. K., & Flamm, R. O. (2003). Conserving manatees: Knowledge, attitudes, and intentions of boaters in Tampa Bay, Florida. *Conservation Biology*, *17*, 1098–1105. https://doi.org/10.1046/j.1523-1739.2003.01452.x

Bauduin, S., Martin, J., Edwards, H. H., Gimenez, O., Koslovsky, S. M., & Fagan, D. E. (2013). An index of risk of co-occurrence between marine mammals and watercraft: Example of the Florida manatee. *Biological Conservation*, *159*, 127–136. https://doi.org/10.1016/j.biocon.2012.10.031

Berkelaar, M. (2015). lpSolve: Interface to 'Lp_solve' v. 5.5 to solve linear/integer programs. R package version 5.6.13.

Calleson, C. S. (2014). Issues and opportunities associated with using manatee mortality data to evaluate the effectiveness of manatee protection efforts in Florida. *Endangered Species Research*, *26*, 127–136. https://doi.org/10.3354/esr00638

Calleson, C. S., & Frohlich, R. K. (2007). Slower boat speeds reduce risks to manatees. *Endangered Species Research*, *3*, 295–304. https://doi.org/10.3354/esr00056

Conn, P. B., & Silber, G. K. (2013). Vessel speed restrictions reduce risk of collision-related mortality for North Atlantic right whales. *Ecosphere*, *4*, 1–16.

Dorazio, R. M., Martin, J., & Edwards, H. H. (2013). Estimating abundance while accounting for rarity, correlated behavior, and other sources of variation in counts. *Ecology*, *94*, 1472–1478. https://doi.org/10.1890/12-1365.1

Edwards, H. H., Martin, J., Deutsch, C. J., Muller, R. G., Koslovsky, S. M., Smith, A. J., & Barlas, M. E. (2016). Influence of manatees' diving on their risk of collision with watercraft. *PLoS ONE*, *11*, e0151450. https://doi.org/10.1371/journal.pone.0151450

Gerritsen, J., & Strickler, J. R. (1977). Encounter probabilities and community structure in zooplankton: A mathematical model. *Journal of the Fisheries Board of Canada*, *34*(1), 73–82. https://doi.org/10.1139/f77-008

Goodwin, P., & Wright, G. (2009). *Decision analysis for management judgment*. New York, NY: John Wiley & Sons Ltd.

Gorzelany, J. F. (2008). Aerial surveys of recreational boating activity in Collier County. Mote Technical Report No. 1259. Sarasota, FL, Mote Marine Laboratory.

Gurarie, E., & Ovaskainen, O. (2013). Towards a general formalization of encounter rates in ecology. *Theoretical Ecology*, *6*, 189–202. https://doi.org/10.1007/s12080-012-0170-4

Haase, C. G., Fletcher, R. J., Slone, D. H., Reid, J. P., & Butler, S. M. (2017). Landscape complementation revealed through bipartite networks: An example with the Florida manatee. *Landscape Ecology*, *32*, 1999–2014. https://doi.org/10.1007/s10980-017-0560-5

Hutchinson, J. M. C., & Waser, P. M. (2007). Use, misuse and extensions of the "ideal gas" models of animal movement. *Biological Reviews*, *82*, 335–359. https://doi.org/10.1111/j.1469-185X.2007.00014.x

Johnson, N. L., Kemp, A. W. & Kotz, S. (2005). *Univariate discrete distributions* (Vol. 444). Hoboken, NJ: John Wiley & Sons.

Kéry, M., & Schaub, M. (2012). *Bayesian population analysis using WinBUGS: A hierarchical perspective*. San Diego, CA: Academic Press.

Koopman, B. O. (1956). The theory of search. I. Kinematic bases. *Operations Research*, *4*, 324–346. https://doi.org/10.1287/opre.4.3.324

Kuchel, P. W., & Vaughan, R. J. (1981). Average lengths of chords in a square. *Mathematics Magazine*, *54*, 261–269. https://doi.org/10.1080/0025570X.1981.11976939

Kunz, T. H., Arnett, E. B., Cooper, B. M., Erickson, W. P., Larkin, R. P., Mabee, T., & Szewczak, J. M. (2007). Assessing impacts of wind-energy development on nocturnally active birds and bats: A guidance document. *Journal of Wildlife Management*, *71*, 2449–2486. https://doi.org/10.2193/2007-270

Laist, D. W., Knowlton, A. R., Mead, J. G., Collet, A. S., & Podesta, M. (2001). Collisions between ships and whales. *Marine Mammal Science*, *17*, 35–75. https://doi.org/10.1111/j.1748-7692.2001.tb00980.x

Laist, D. W., & Shaw, C. (2006). Preliminary evidence that boat speed restrictions reduce deaths of Florida manatees. *Marine Mammal Science*, *22*, 472–479. https://doi.org/10.1111/j.1748-7692.2006.00027.x

Martin, J., Edwards, H. H., Fonnesbeck, C. J., Koslovsky, S. M., Harmak, C. W., & Dane, T. M. (2015). Combining information for monitoring at large spatial scales: First statewide abundance estimate of the Florida manatee. *Biological Conservation*, *186*, 44–51. https://doi.org/10.1016/j.biocon.2015.02.029

Martin, J., Sabatier, Q., Gowan, T. A., Giraud, C., Gurarie, E., Calleson, C. S., ... Koslovsky, S. M. (2016). A quantitative framework for investigating risk of deadly collisions between marine wildlife and boats. *Methods in Ecology and Evolution*, *7*, 42–50. https://doi.org/10.1111/2041-210X.12447

Moilanen, A., Wilson, K. A., & Possingham, H. (2009). *Spatial conservation prioritization: Quantitative methods and computational tools*. Oxford, UK: Oxford University Press.

Nocedal, J., & Wright, S. (2006). *Numerical optimization*. Berlin, Germany: Springer Science & Business Media.

Plummer, M. (2015). JAGS version 4.0. User manual.

Plummer, M. (2016). rjags: Bayesian graphical models using MCMC. R package version 4-6. Retrieved from https://CRAN.R-project.org/package=rjags

R Core Team. (2016). *R: A language and environment for statistical computing*. Vienna, Austria: R Foundation for Statistical Computing.

Runge, M. C., Sanders-Reed, C. A., Langtimm, C. A., Hostetler, J. A., Martin, J., Deutsch, C. J., ... Mahon, G. L. (2017). Status and threats analysis for the Florida manatee (*Trichechus manatus latirostris*), 2016: U.S. Geological Survey Scientific Investigations Report 2017–5030. 40 p.

Udell, B. J., Martin, J., Fletcher, R. J., Bonneau, M., Edwards, H., Gowan, T., ... Deutsch, C. J. (2018). Data from: Integrating encounter theory with decision analysis to evaluate collision risk and determine optimal protection zones for wildlife. *Dryad Digital Repository*, https://doi.org/10.5061/dryad.7dh4312

United States Fish and Wildlife Service. (2001). *Florida manatee recovery plan*, *(Trichechus manatus latirostris), third revision*. Atlanta, GA: US Fish and Wildlife Service.

van der Hoop, J. M., Vanderlaan, A. S. M., & Taggart, C. T. (2012). Absolute probability estimates of lethal vessel strikes to North Atlantic right whales in Roseway Basin, Scotian Shelf. *Ecological Applications*, *22*, 2021–2033. https://doi.org/10.1890/11-1841.1

Vanderlaan, A. S. M., Corbett, J. J., Green, S. L., Callahan, J. A., Wang, C., Kenney, R. D., ... Firestone, J. (2009). Probability and mitigation of vessel encounters with North Atlantic right whales. *Endangered Species Research*, *6*, 273–285. https://doi.org/10.3354/esr00176

Vanderlaan, A. S. M., & Taggart, C. T. (2007). Vessel collisions with whales: The probability of lethal injury based on vessel speed. *Marine Mammal Science*, *23*, 144–156. https://doi.org/10.1111/j.1748-7692.2006.00098.x

SUPPORTING INFORMATION

Additional supporting information may be found online in the Supporting Information section at the end of the article.

How to cite this article: Udell BJ, Martin J, Fletcher Jr RJ, et al. Integrating encounter theory with decision analysis to evaluate collision risk and determine optimal protection zones for wildlife. *J Appl Ecol*. 2019;56:1050–1062. https://doi.org/10.1111/1365-2664.13290